

Earth and Space Science

RESEARCH ARTICLE

10.1029/2021EA001958

Key Points:

- We measure the amplitude distribution of lightning very high frequency (VHF) pulses
- The VHF pulse amplitude spectrum follows a power-law
- The top 10-percentile amplitude decreases with altitude

Correspondence to:

J. G. O. Machado,
j04ogm@gmail.com

Citation:

Machado, J. G. O., Hare, B. M., Scholten, O., Buitink, S., Corstanje, A., Falcke, H., et al. (2022). The relationship of lightning radio pulse amplitudes and source altitudes as observed by LOFAR. *Earth and Space Science*, 9, e2021EA001958. <https://doi.org/10.1029/2021EA001958>

Received 10 AUG 2021

Accepted 12 OCT 2021

Author Contributions:

Conceptualization: J. G. O. Machado, B. M. Hare, O. Scholten

Data curation: J. G. O. Machado, B. M. Hare, O. Scholten, S. Buitink, A. Corstanje, H. Falcke, J. R. Hörandel, T. Huege, G. K. Krampah, P. Mitra, K. Mulrey, A. Nelles, H. Pandya, J. P. Rachen, S. Thoudam, T. N. G. Trinh, S. ter Veen, T. Winchen

Formal analysis: J. G. O. Machado, B. M. Hare, O. Scholten

Funding acquisition: J. G. O. Machado, B. M. Hare, O. Scholten, S. Buitink, A. Corstanje, H. Falcke, J. R. Hörandel, T. Huege, G. K. Krampah, P. Mitra, K. Mulrey, A. Nelles, H. Pandya, J. P. Rachen, S. Thoudam, T. N. G. Trinh, S. ter Veen, T. Winchen

Investigation: J. G. O. Machado, B. M. Hare, O. Scholten





Methodology: J. G. O. Machado, B. M. Hare, O. Scholten

Project Administration: B. M. Hare, O. Scholten, S. Buitink, A. Corstanje, H.

© 2021 The Authors.

This is an open access article under the terms of the [Creative Commons Attribution-NonCommercial License](#), which permits use, distribution and reproduction in any medium, provided the original work is properly cited and is not used for commercial purposes.

The Relationship of Lightning Radio Pulse Amplitudes and Source Altitudes as Observed by LOFAR

J. G. O. Machado¹ , B. M. Hare² , O. Scholten^{2,3}, S. Buitink^{4,5}, A. Corstanje^{4,5}, H. Falcke^{4,6,7}, J. R. Hörandel^{4,5,6}, T. Huege^{5,8}, G. K. Krampah⁵, P. Mitra⁵, K. Mulrey⁵, A. Nelles^{9,10}, H. Pandya⁵ , J. P. Rachen⁵, S. Thoudam¹¹, T. N. G. Trinh¹² , S. ter Veen^{4,7}, and T. Winchen¹³

¹Physics Institute, University of Brasilia, Brasilia, Brazil, ²Kapteyn Astronomical Institute, University of Groningen, Groningen, The Netherlands, ³Interuniversity Institute for High-Energy, Vrije Universiteit Brussel, Brussels, Belgium, ⁴Department of Astrophysics/IMAPP, Radboud University Nijmegen, Nijmegen, The Netherlands, ⁵Astrophysical Institute, Vrije Universiteit Brussel, Brussels, Belgium, ⁶NIKHEF, Science Park Amsterdam, Amsterdam, The Netherlands, ⁷Netherlands Institute of Radio Astronomy (ASTRON), Dwingeloo, The Netherlands, ⁸Institute for Astroparticle Physics (IAP), Karlsruhe Institute of Technology (KIT), Karlsruhe, Germany, ⁹DESY, Zeuthen, Germany, ¹⁰ECAP, Friedrich-Alexander-University Erlangen-Nrnberg, Erlangen, Germany, ¹¹Department of Physics, Khalifa University, Abu Dhabi, United Arab Emirates, ¹²Department of Physics, School of Education, Can Tho University Campus II, Can Tho City, Vietnam, ¹³Max-Planck-Institut für Radioastronomie, Bonn, Germany

Abstract When a lightning flash is propagating in the atmosphere it is known that especially the negative leaders emit a large number of very high frequency (VHF) radio pulses. It is thought that this is due to streamer activity at the tip of the growing negative leader. In this work, we have investigated the dependence of the strength of this VHF emission on the altitude of such emission for two lightning flashes as observed by the Low Frequency ARray (LOFAR) radio telescope. We find for these two flashes that the extracted amplitude distributions are consistent with a power-law, and that the amplitude of the radio emissions decreases very strongly with source altitude, by more than a factor of 2 from 1 km altitude up to 5 km altitude. In addition, we do not find any dependence on the extracted power-law with altitude, and that the extracted power-law slope has an average around 3, for both flashes.

1. Introduction

A negative leader propagates in a stepping fashion where the leader halts in between forward jumps. In between the forward jumps the corona at the leader tip gradually charges up until the corona explodes forward in a corona burst, emitting strong very high frequency (VHF) pulses. A corona is a region of very weakly conducting plasma around a leader, generally thought to consist of many streamers where a streamer is a self-propagating structure which develops inside a charged region (Dwyer & Uman, 2014). It is thought that VHF (30–300 MHz) radio emission from lightning is dominated by streamer activity (Hare et al., 2020; Scholten et al., 2021; Scholten, Hare, Dwyer, Liu, et al., 2021; Shi et al., 2019). A corona burst thus emits VHF radiation most profusely because many streamers are initiated. Since streamers can be thought of as a moving head of charge, the emission from a streamer is roughly proportional to the charge of the streamer times its acceleration.

From laboratory experiments (Li et al., 2016; Nijdam et al., 2020) it is known that the streamer activity depends strongly on air density, in particular (Briels et al., 2008; Huiskamp et al., 2013) have shown that streamer propagation speed increases with decreasing air density. Assuming that the initial acceleration of a streamer is related to its top propagation velocity, and since the streamers a corona burst accelerate to top speed quickly, it could be expected that the VHF emission from lightning should increase with altitude since the top speed should increase with altitude. However, in the laboratory experiments of (Li et al., 2016), it is shown that the time duration of the corona current pulse increases much faster than linear with decreasing air pressure when keeping the same ratio between applied voltage and onset voltage. This implies that the time-derivative of the corona current, and thus the VHF emission, should strongly decrease with altitude, in sharp contrast to the previously suggested model.

Therefore, in this work we explore how the amplitude of VHF emission from lightning, which is believed to be dominated by streamer activity (Hare et al., 2020; Scholten et al., 2021; Scholten, Hare, Dwyer, Liu, et al., 2021; Shi et al., 2019) varies with altitude, and thus air pressure, in an attempt to better understand streamer dynamics and guide future modeling.

Falcke, J. R. Hörandel, T. Huege, G. K. Krampah, P. Mitra, K. Mulrey, A. Nelles, H. Pandya, J. P. Rachen, S. Thoudam, T. N. G. Trinh, S. ter Veen, T. Winchen
Resources: J. G. O. Machado, B. M. Hare, O. Scholten, S. Buitink, A. Corstanje, H. Falcke, J. R. Hörandel, T. Huege, G. K. Krampah, P. Mitra, K. Mulrey, A. Nelles, H. Pandya, J. P. Rachen, S. Thoudam, T. N. G. Trinh, S. ter Veen, T. Winchen
Software: J. G. O. Machado, B. M. Hare, O. Scholten, S. Buitink, A. Corstanje, H. Falcke, J. R. Hörandel, T. Huege, G. K. Krampah, P. Mitra, K. Mulrey, A. Nelles, H. Pandya, J. P. Rachen, S. Thoudam, T. N. G. Trinh, S. ter Veen, T. Winchen
Supervision: B. M. Hare, O. Scholten
Validation: J. G. O. Machado, B. M. Hare, O. Scholten
Visualization: J. G. O. Machado, B. M. Hare, O. Scholten
Writing – original draft: J. G. O. Machado
Writing – review & editing: J. G. O. Machado, B. M. Hare, O. Scholten, S. Buitink, A. Corstanje, H. Falcke, J. R. Hörandel, T. Huege, G. K. Krampah, P. Mitra, K. Mulrey, A. Nelles, H. Pandya, J. P. Rachen, S. Thoudam, T. N. G. Trinh, S. ter Veen, T. Winchen

2. Methods

We investigated two lightning flashes, one from September 29, 2017 at 17:34:55 UTC, and another from August 13, 2018 at 15:30:01 UTC, referred to as the “2017” and “2018” flashes respectively, that were detected by Low Frequency ARray (LOFAR) and imaged as described in Section 2.1. In order to investigate the effect of altitude (pressure) on the VHF emission of lightning, we selected negative leaders from these two flashes and found the distribution of recorded pulse peak amplitudes at different altitudes with 500 m tall altitude bins. For the VHF-sources located on negative leaders within a certain altitude range we determined the distributions of peak amplitudes in a reference antenna. These distributions are analyzed in Section 2.2.

2.1. Lightning Imaging and the LOFAR Radio Telescope

The LOFAR is a high precision radio telescope capable of locating lightning VHF sources with 10 ns temporal precision. It consists of over 4,512 low-band antennas and 2,256 high-band antennas distributed within dozens of stations scattered across the northern Netherlands. There are also international stations in other European countries, but they are not used for mapping lightning. For lightning observations we use the low-band antennas operating over the 10 ~ 90 MHz range (van Haarlem et al., 2013). LOFAR's high temporal and spatial precision and its low noise level makes it possible to detect many more pulses than any other antenna array, such as a Large Millimeter Array, and view in detail negative leaders stepping process (Hare et al., 2019, 2020).

Figure 1 shows typical lightning VHF waveform as detected by LOFAR, and illustrates the pulse detection algorithm used in this work. The pulse detection algorithm works top-down. For each section of data to be analyzed (generally processed in 330 μ s chunks) the algorithm picks the strongest local maxima in that time trace. A 10 sample (50 ns) wide window is then centered on this local maxima. This process is then repeated for the rest of the waveform but excluding that data inside other windows. Thus, the windows around each peak are allowed to overlap, but each window is only allowed to contain one peak (as shown in Figure 1). This process is repeated until all pulses above a threshold are found. This threshold is set to 3 SDs of the noise. Note that this noise can only truly be measured when there is no lightning, thus Figure 1 does not contain any pure noise. The peaks detected in this procedure we refer to as “detected” pulses in this work. After pulse detection on a central reference antenna, we attempt to image and locate the source region using the techniques described in Scholten, Hare, Dwyer, Sterpka, et al. (2021). We are only able to locate some of the detected pulses, which we refer to as “imaged” or “located” pulses in this work. The lightning pulses observed by LOFAR are extremely similar to the impulse response function of the LOFAR antennas, and thus the frequency spectrum is fairly flat in LOFAR's frequency band. Therefore, any attempt to extract information from the frequency spectra would need to explore very subtle effects and would be prone to instrumental artifacts. Thus, in this work we only consider the pulse amplitude and source location. Imaged source locations are depicted in Figures 2 and 3, which shows the image of the 2017 and 2018 flashes, respectively, with the negative leaders used in this work indicated.

2.2. Analysis of Pulse Amplitudes

As demonstrated in Figure 1, VHF radiation from lightning, as observed by LOFAR, is extremely impulsive, where each recorded pulse has a full-width-half-max (FWHM) of around 50 ns. As a proxy for the amplitude of each radio source, the peak amplitude of the pulse is taken as recorded by a central antenna, called the reference antenna. Since we are only interested in how the amplitude changes with source altitude, we have not performed any absolute calibration, and only present the amplitudes as measured by the digitizer. Thus, we do not need to account for pulse attenuation due to distance from the source, as we will discuss more below. The negative leaders from the two flashes we consider in this work were arranged in 500 m tall altitude bins and for each bin the strength distribution of the sources is analyzed.

The efficiency of our imaging algorithm depends on pulse strength; strong pulses clearly stick out and are thus more easily detected and significantly more easily located than weaker ones. This potentially introduces a pulse-amplitude dependent bias. To explore this, Figure 4 compares the amplitude distribution of detected and imaged radio pulses between times $t = 100$ ms and $t = 150$ ms from the 2017 flash shown in Figure 2. We have made this selection because there was very little activity elsewhere during this time, and because the negative leaders occurred over a relatively narrow altitude range. For most other cases this comparison cannot be made

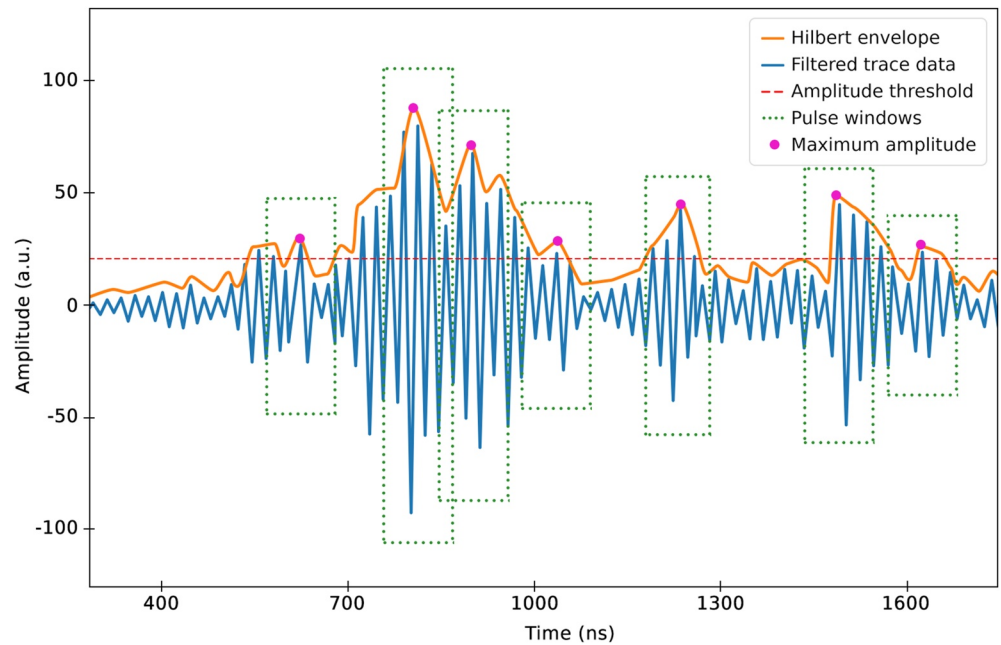


Figure 1. A filtered trace from the data with its Hilbert envelope. The dotted green line depicts the windows for the pulse detection algorithm, which are 10 samples wide, and the pink points show the peak amplitudes inside each window. The threshold for pulse detection is set at an amplitude of 15 which is about 3 SDs from the noise baseline. Amplitude is given in arbitrary units.

as there is lightning activity at many different altitudes and it is necessary to locate the source. As expected, the source locations could be found for almost all strong peaks and pulse-imaging efficiency becomes gradually worse for the weaker pulses. This is also expressed in the lower panel of Figure 4, showing that the ratio between the two amplitude distributions (number of located divided by the number of all detected pulses) is fairly constant and close to unity for the strongest 10% pulses. The error bars in Figure 4 indicate the statistical uncertainty, and thus are largest for the highest amplitude bins that have the fewest number of counts. The error bars in the top panel are simply $\sigma(n) = \sqrt{n}$, where n is the number of pulses. The error bars in the bottom panel are simply propagated through the division and thus are $\sigma(n_d/n_i) = (n_d/n_i) \sqrt{(\sigma(n_d)/n_d)^2 + (\sigma(n_i)/n_i)^2}$.

In addition to the imaging efficiency, Figure 4 allows us to observe the shape of the amplitude distribution. To do this, one should only consider the top 10% of sources as they are minimally affected by the instrument. This 10% cutoff is shown in Figure 4 as a vertical bar for the detected and imaged pulses. Figure 4 shows that the log of the bin heights decreases linearly with amplitude and is thus follows a power law distribution. This observation of a power law of the highest amplitude pulses is consistent across all data we have examined. This power law distribution is fascinating as it must be a direct result of the underlying physics, but what physical processes should be at work here is not clear and should be explored in future work. In addition, this observation of power law distributions makes the interpretation of this work slightly more challenging, as power laws are particularly mathematically pathological.

To characterize the pulse distribution at large amplitudes we explored two different statistics. First, the absolute pulse strength is characterized by the 10-percentile amplitude. We choose this statistic because the maximum amplitude for a stochastic process will increase with the number of analyzed pulses while a percentile value is more stable. We have opted for the 10% amplitude since this is the largest percentile that is not much affected by the imaging efficiency as seen from Figure 4. The two vertical bars in Figure 4 show the 10% cut amplitude for the imaged and detected pulses. Due to the smaller imaging efficiency at smaller amplitudes the 10% value for the detected pulses is somewhat smaller than for the imaged sources. However we do not expect this to significantly influence our results as a similar effect is observed on amplitude distributions for all analyzed data. In addition we also report the power law slope λ of a power-law fitted to the strongest 10% of events,

$$N(a) = N_0 a^{-\lambda}, \quad (1)$$

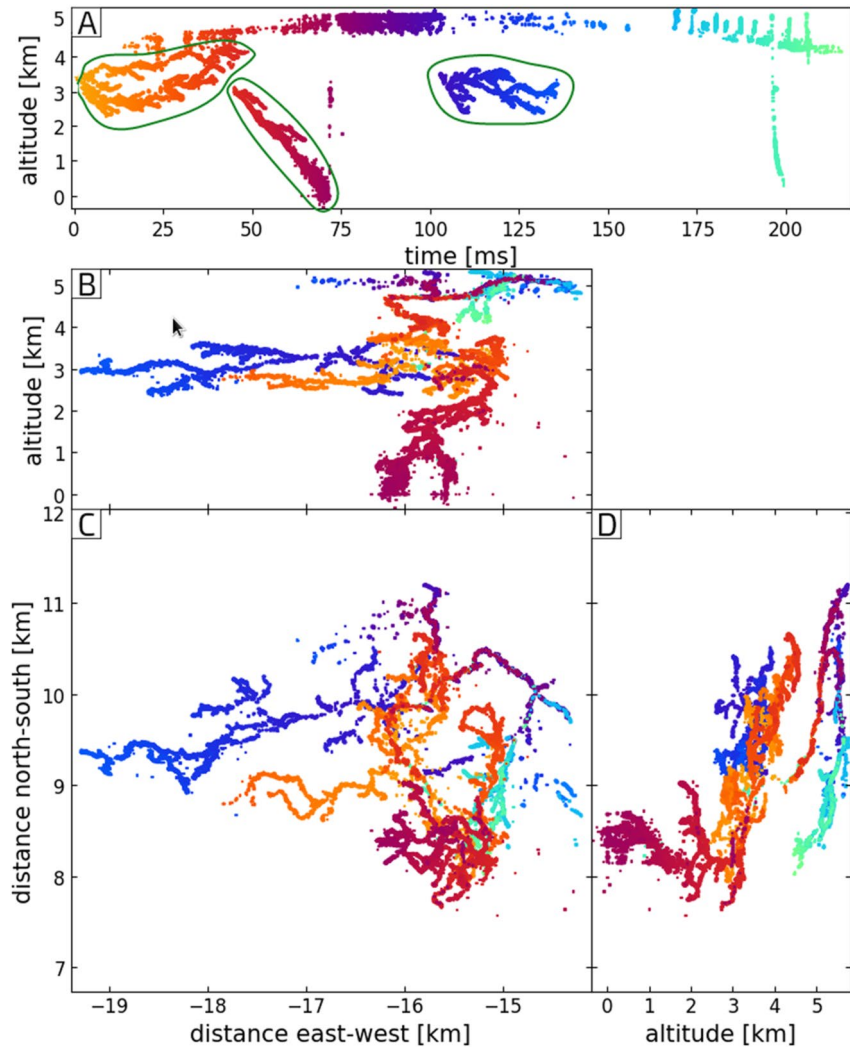


Figure 2. Plan view of the 2017 flash imaged data, colored by time. Each point represents a located VHF source. Negative leaders are circled in green. The figure panels are: (a) time versus altitude (from ground), (b) east-west distance (from core center) versus altitude, (c) east-west distance (from core center) versus north-south (from core center), and (d) altitude (from ground) versus east-west distance (from core center).

where $N(a)$ is the number of events at amplitude a and N_0 is a normalization factor. As illustrated by the slanted lines in Figure 4 λ was extracted by first binning the pulse amplitudes (with logarithmic bin widths), and we then only used the bins that contained the top 10% of pulses. The \log_{10} of the number of sources in those top bins was fitted with a line such that the slope of the line is λ .

2.3. Correction Factors

There are several factors that affect the relationship between the detected pulse amplitude and the actual emitted amplitude. Some of these will be important for the altitude dependence we investigate in this work.

Since an impulsive source is likely driven by a rapidly changing current with a certain orientation, the VHF emission will have an angle-dependent emission pattern, likely similar to dipole emission. This will potentially affect the detected strength. However, since we consider the emission from many sources that are likely to have random orientations, the affect of the emission pattern is not altitude-dependant and thus does not affect the conclusions of our work. The only way in which the source emission pattern could affect our conclusions is if the distribution of streamer directions changes with altitude. In our data, the negative leaders are mostly horizontal above 2 km

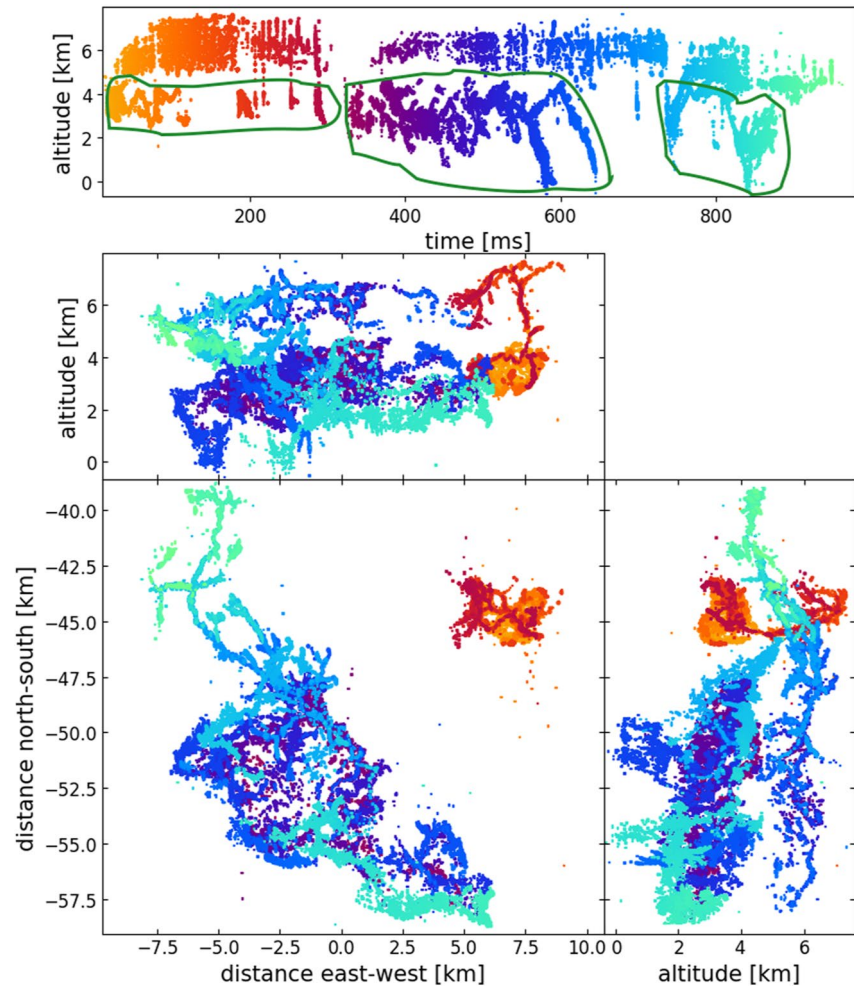


Figure 3. Plan view of the 2018 flash imaged data, colored by time. Each point represents a located VHF source. Negative leaders are circled in green. The figure panels are: (a) time versus altitude (from ground), (b) east-west distance (from core center) versus altitude, (c) east-west distance (from core center) versus north-south (from core center), and (d) altitude (from ground) versus east-west distance (from core center).

altitude and mostly vertical below 2 km altitude. Thus, if we imagine an extreme scenario where all the streamers above 2 km altitude are purely horizontal and those below 2 km altitude are purely vertical then there could be an altitude-dependent amplitude change up to a factor of $\sqrt{2}$ (based on dipole emission pattern considerations) that is due to streamer orientation and not streamer physics. This is discussed further in Section 3.

Sources that are further away will have weaker recorded amplitudes in the reference antenna. This, however, is not a significant concern as the spatial extent of each of the two flashes (≈ 5 km for 2017 flash and ≈ 20 km for the 2018 flash) is smaller than the distance to the flash itself (≈ 18.6 km for 2017 flash and ≈ 50 km for the 2018 flash). Therefore, while our measured amplitudes cannot be compared between flashes, the shape of the amplitude distribution should be robust to distance variations within each lightning flash. Thus, we do not account for pulse attenuation due to distance in this early work.

More importantly, however, are the effects of LOFAR's antenna function. Radio emission from different sources will arrive from different elevation (θ_e) and azimuth (ϕ) angles, and therefore will be amplified differently by the antenna function. The azimuth-angle dependence is not very strong as all sources are in a small angular regime where the antenna function is large. Particular care needs to be given to the elevation angle as the LOFAR antennas have vanishing sensitivity for sources at $\theta_e = 0$. Basic analytic considerations for the angular dependence of the measured amplitude one thus concludes that the antenna function is proportional to $\sin(\theta_e)$ for the small values of θ_e that are relevant for this work. Since $\sin(\theta_e) \approx \tan(\theta_e) = h/R$, where h is the altitude of the source and

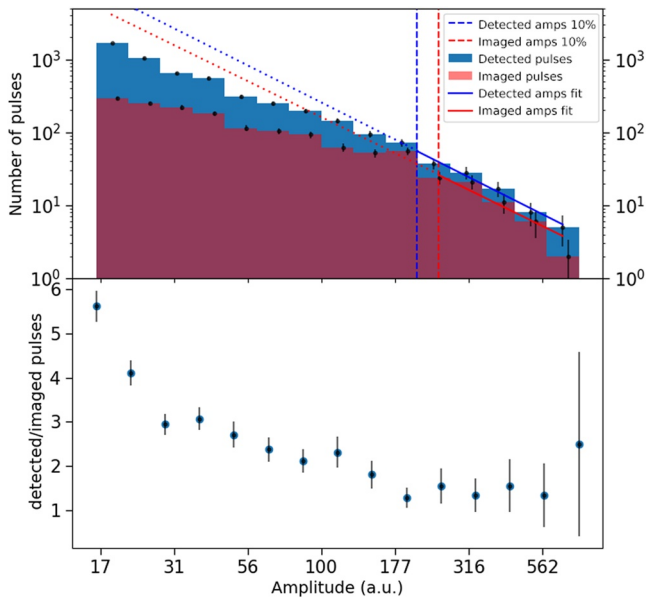


Figure 4. The upper image shows on a log-log scale a comparison between the distributions of amplitudes (amps on the legend) of located sources and all pulses as detected in the reference antenna between times $t = 100$ ms and $t = 150$ ms from the 2017 flash. The solid lines show a power-law fit to the strongest 10% of sources with the dotted part regarding its extrapolation below the 10% line, and the vertical bar shows the 10% amplitude. The power-law slope, λ , for both fits is 2.32. The lower panel depicts the ratio of the number of located and all pulses per amplitude bin. Amplitude is in arbitrary units.

Table 1
The Parameters for the Amplitude Distributions for Negative Leaders at Different Altitude Sections for the Two Flashes Considered in This Work

Altitude	2017 flash				2018 flash			
	Sources	a_{10}^d	a_{10}^c	λ	sources	a_{10}^d	a_{10}^c	λ
0.0–0.5 km	353	137	2,740	3.62	74	99	1,980	4.64
0.5–1.0 km	1,077	215	1,433	2.42	110	93	620	2.50
1.0–1.5 km	910	255	1,020	1.73	368	102	408	2.85
1.5–2.0 km	1,643	292	834	2.45	721	116	331	4.03
2.0–2.5 km	1,496	311	691	2.28	893	123	273	4.46
2.5–3.0 km	3,714	312	567	2.90	1,866	137	249	3.42
3.0–3.5 km	3,110	322	795	2.93	2,818	149	229	3.31
3.5–4.0 km	1,709	324	432	2.11	3,434	162	216	3.51
4.0–4.5 km	652	286	336	2.65	2,048	166	195	2.48
4.5–5.0 km					429	200	210	1.82
5.0–5.5 km					25	156	148	1.05

Note. The first column is the altitude range. For each flash the first gives the number of sources in the negative leader at that altitude, the second column gives the 10-percentile value of the measured amplitude, which is corrected for the effects of the antenna function in the third column, and the last column gives the the power-law slope, λ .

R the distance. This correction is included in the results on Table 1. Further detailed description of LOFAR antennas functionality is given by (Nelles et al., 2015).

3. Results and Discussion

Table 1 shows the results for the extracted statistics on the pulse distributions for the 2017 and 2018 flashes, respectively. For each we give, the altitude range, the number of located sources, the 10% percentile amplitude a_{10}^d , the same value corrected for the antenna function a_{10}^c , and the fitted power-law slope. As we have argued in Section 2.3 the correction of the pulse strength is inversely proportional to the altitude of the source. Normalizing the correction to unity at 5 km we thus obtain

$$a_{10}^c = \frac{5}{h} a_{10}^d, \quad (2)$$

where h is the mean altitude of the bin in units of km.

For these two flashes our data show that the a_{10}^d values tends to increase slowly with altitude, however, when corrected for the antenna function, a_{10}^c , the values rapidly decrease with altitude as can be seen from Figure 5. This shows that the peak amplitudes of individual VHF pulses decrease strongly with increasing altitude for these two flashes for leaders below 5 km altitude. These early results demonstrate the ability to explore the properties of VHF emission to much higher detail than possible before. Since these two flashes have a distinct development and occurred in different contexts (being observed a year apart), this implies that the observed strong amplitude fall-off with altitude could be general. This will be explored in future work. Previous studies (Chmielewski & Bruning, 2016), has suggested that flash size could impact the overall VHF magnitude of a lightning flash. Unfortunately, in this early work we were unable to explore the difference in overall magnitude between the two lightning flashes. Since recent work (Hare et al., 2020; Scholten et al., 2021; Shi et al., 2019) has strongly suggested that VHF emission from lightning comes from streamers, we believe that our observed VHF peak amplitudes are indicative of lightning streamer amplitudes.

As discussed in Section 2.3, since negative leaders we have analyzed at lower altitudes are mostly vertical and the ones at higher altitudes are mostly horizontal, the fact that the streamer directions are not randomly oriented may seem to be a problem. However, our results show that the amplitude can change by a factor of 5–8 from ground to cloud level, which is significantly larger than the $\sqrt{2}$ that could be created by different streamer orientations. Thus, our results are too strong to be explained by a streamer orientation distribution that varies with altitude.

The results from laboratory streamer experiments as reported in Li et al. (2016) indicate that, for a fixed value of the electric field over breakdown, the current in a streamer decreases with decreasing pressure while at the same time also the width of the current pulse increases. Figure 6 of Li et al. (2016) indicates that the pulse-width increases by about a factor of 3 when the pressure halves. Since the radiated power is expected to be proportional to the current-change, we thus expect the radiated power to decrease strongly with increasing altitude like is shown from our results. However, the strong increase of pulse strength toward lower altitudes appears not consistent with laboratory results and rather suggests that the proximity of the

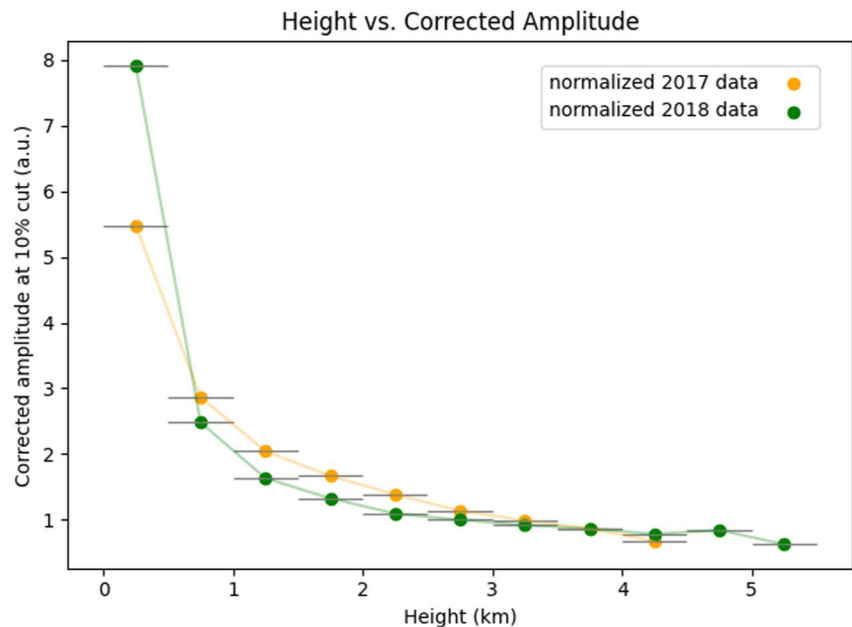


Figure 5. The altitude dependence of the corrected 10-percentile amplitudes (a_{10}^c from Table 1) are shown for the two flashes. The values for the two flashes have been normalized to each other for the 2.5–3.0 km altitude bin. The vertical error bar indicates the bin size in altitude.

ground is important. It is important to stress the statistical reliability and resolution provided by LOFAR, and also the fact that the amplitude for each pulse is computed individually, and not the emitted radiation as a whole.

Another possible interpretation is that at low altitudes the VHF-emission is enhanced due to the proximity of the ground via image-charge effects, which may explain the strong increase of the emission below 1 km altitude.

Another interesting observation is that the amplitude distributions we have found at the highest amplitudes (where imaging efficiency is constant) shows an approximately linear dependency on a double log-scale. This strongly implies that the amplitude distribution follows a power law, which is scale invariant. The values for this power, as shown in Table 1, vary considerably, probably due to poor statistics, but seem to have a mean value of about 3. No distinct altitude dependence is shown by the results. In a future work, we will investigate this in more detail.

Data Availability Statement

The data for the figures can be found at Machado et al. (2021). The raw LOFAR data are available from the LOFAR Long Term Archive (for access see ASTRON [2020]). To download this data, please create an account and follow the instructions for “Staging Transient Buffer Board data” at ASTRON (2020). In particular, the utility “wget” should be used as follows: wget <https://lofar-download.grid.surfsara.nl/lofigrid/SRMFFifoGet.py?url='location'> where “location” should be specified as: <https://srm.grid.sara.nl/pnfs/grid.sara.nl/data/lofar/ops/TBB/lightning/> followed by: L612746_D20170929T202255.000Z_“stat”_R000_tbb.h5 (for the 2017 Flash), D20180813T153001.413Z_“stat”_R000_tbb.h5 (for the 2018 Flash), and where “stat” should be replaced by the name of the station: CS001, CS002, CS003, CS004, CS005, CS006, CS007, CS011, CS013, CS017, CS021, CS024, CS026, CS028, CS030, CS031, CS032, CS101, CS103, RS106, CS201, RS205, RS208, RS210, CS301, CS302, RS305, RS306, RS307, RS310, CS401, RS406, RS407, RS409, CS501, RS503, RS508, or RS509.

References

- ASTRON. (2020). *LOFAR long term archive access*. Retrieved from https://www.astron.nl/lofarwiki/doku.php?id=public:ita_howto
- Briels, T., van Veldhuizen, E., & Ebert, U. (2008). Positive streamers in air and nitrogen of varying density: Experiments on similarity laws. *Journal of Physics D*, 41, 234008. <https://doi.org/10.1088/0022-3727/41/23/234008>
- Chmielewski, V. C., & Bruning, E. C. (2016). Lightning mapping array flash detection performance with variable receiver thresholds. *Journal of Geophysical Research: Atmospheres*, 121(14), 8600–8614. <https://doi.org/10.1002/2016JD025159>

Acknowledgments

This study was financed in part by the Coordenação de Aperfeiçoamento de Pessoal de Nível Superior Brasil (CAPES) Finance Code 001 and by the Fundação de Apoio Pesquisa do Distrito Federal - FAP/DF. The LOFAR cosmic-ray key science project acknowledges funding from an Advanced Grant of the European Research Council (FP/2007–2013) / ERC Grant Agreement no. 227610. The project has also received funding from the European Research Council (ERC) under the European Unions Horizon 2020 research and innovation programme (grant agreement No 640130). The authors furthermore acknowledge financial support from FOM, (FOM-project 12PR304). S. Thoudam acknowledges funding from the Khalifa University Startup grant (project code 8474000237). B. M. Hare is supported by NWO (VI.VENI.192.071). K. Mulrey is supported by FWO (FWO-12ZD920N). A. Nelles acknowledges the DFG grant NE 2031/2-1. T. N. G. Trinh acknowledges funding from the Vietnam National Foundation for Science and Technology Development (NAFOSTED) under (Grant number 103.01-2019.378). LOFAR, the Low Frequency Array designed and constructed by ASTRON, has facilities in several countries, that are owned by various parties (each with their own funding sources), and that are collectively operated by the International LOFAR Telescope foundation under a joint scientific policy.

- Dwyer, J. R., & Uman, M. A. (2014). The physics of lightning. *Physics Reports*, 534(4), 147–241. <https://doi.org/10.1016/j.physrep.2013.09.004>
- Hare, B. M., Scholten, O., Dwyer, J., Ebert, U., Nijdam, S., Bonardi, A., et al. (2020). Radio emission reveals inner meter-scale structure of negative lightning leader steps. *Physical Review Letters*, 124, 105101. <https://doi.org/10.1103/PhysRevLett.124.105101>
- Hare, B. M., Scholten, O., Dwyer, J., Trinh, T. N. G., Buitink, S., ter Veen, S., et al. (2019). Needle-like structures discovered on positively charged lightning branches. *Nature*, 568, 360–363. <https://doi.org/10.1038/s41586-019-1086-6>
- Huiskamp, T., Pemen, A., Hoeben, W., Beckers, F., & van Heesch, E. (2013). Temperature and pressure effects on positive streamers in air. *Journal of Physics D*, 46, 165202. <https://doi.org/10.1088/0022-3727/46/16/165202>
- Li, X., Cui, X., Lu, T., Li, D., Chen, B., & Fu, Y. (2016). Influence of air pressure on the detailed characteristics of corona current pulse due to positive corona discharge. *Physics of Plasmas*, 23(12), 123516. <https://doi.org/10.1063/1.4971804>
- Machado, J., Scholten, O., Hare, B., Buitink, S., Corstanje, A., Falcke, H., et al. (2021). Processed Data for “The relationship of lightning radio pulse amplitudes and source altitudes as observed by LOFAR”. *Earth and Space Science Open Archive ESSOAr*. <https://doi.org/10.34894/XXWHFV>
- Nelles, A., Hörandel, J. R., Karskens, T., Krause, M., Buitink, S., Corstanje, A., et al. (2015). Calibrating the absolute amplitude scale for air showers measured at LOFAR. *Journal of Instrumentation*, 10. <https://doi.org/10.1088/1748-0221/10/11/P11005>
- Nijdam, S., Teunissen, J., & Ebert, U. (2020). The physics of streamer discharge phenomena. *Plasma Sources Science and Technology*, 29(10), 103001. <https://doi.org/10.1088/1361-6595/abaa05>
- Scholten, O., Hare, B., Dwyer, J., Liu, N., Sterpka, C., Buitink, S., & Winchen, T. (2021). Distinguishing features of high altitude negative leaders as observed with LOFAR. *Atmospheric Research*, 260, 105688. <https://doi.org/10.1016/j.atmosres.2021.105688>
- Scholten, O., Hare, B. M., Dwyer, J., Liu, N., Sterpka, C., Buitink, S., et al. (2021). Time resolved 3D interferometric imaging of a section of a negative leader with LOFAR. *Physical Review D*. <https://doi.org/10.1103/physrevd.104.063022>
- Scholten, O., Hare, B. M., Dwyer, J., Sterpka, C., Kolmasova, I., Santolik, O., & Winchen, T. (2021). The initial stage of cloud lightning imaged in high-resolution. *Journal of Geophysical Research: Atmospheres*, 126(4), e2020JD033126. <https://doi.org/10.1029/2020jd033126>
- Shi, F., Liu, N., Dwyer, J. R., & Ihaddadene, K. M. A. (2019). VHF and UHF electromagnetic radiation produced by streamers in lightning. *Geophysical Research Letters*, 46(1), 443–451. <https://doi.org/10.1029/2018gl080309>
- van Haarlem, M. P., Wise, M. W., Gunst, A. W., Heald, G., McKean, J. P., Hessels, J. W. T., et al. (2013). LOFAR: The low-frequency array. *Astronomy & Astrophysics*, 556(A2). <https://doi.org/10.1051/0004-6361/201220873>